HIGH LIFT RESEARCH AND ITS APPLICATION TO AIRCRAFT DESIGN

J.R. Wedderspoon
Head of Fluid Mechanics,
British Aerospace, Aircraft Group,
Weybridge-Bristol Division,
Weybridge,
Surrey.

ABSTRACT

The aerodynamic research and development procedures used by the Weybridge-Bristol Division of British Aerospace to design efficient high lift devices for advanced civil transport aircraft are described, stressing the importance of achieving the correct balance between theory and experiment. The theoretical methods used are reviewed, and the design of a rigid Kruger slat is discussed. The main experimental techniques are described and the importance of the large body of data obtained during a major U.K. research programme the 'National High Lift Programme' is assessed. Some interesting results from this programme are quoted including the effect of supercritical section profiles on high lift performance.

1. INTRODUCTION

The research and development required to design efficient high lift devices for advanced civil transport aircraft generally involves a complex blend of theoretical research, experimental evaluation in two dimensions, followed by the final implementation in three dimensions. The objective of the best possible aerodynamic efficiency must always be weighed against the requirements of good handling characteristics at the stall, and the problems of practical slat and flap track support systems must also be considered.

In this paper the high lift research and development procedures used by the Weybridge-Bristol Division of British Aerospace are described stressing the importance of the balance between theory and experiment.

The theoretical methods used are reviewed. In two dimensions these range from simple surface singularity methods to viscous interactive solutions and as an example, the design of a rigid Kruger slat is described. In three dimensions the possibilities for using quasi three-dimensional theory to optimise the high lift system across the span are examined.

Experimental techniques are next discussed, with particular reference to the large two dimensional and quasi two-dimensional models developed as part of the U.K. National High Lift Programme. A large number of both conventional and advanced high lift devices were developed using these models and some interesting results are shown. These include comparisons between a rigid Kruger slat and an over wing slat, a comparison between an externally hinged flap system and a tracked system, and the effect of modifying a conventional section to have supercritical section profiles.

Three-dimensional experimental procedures are discussed, stressing the complexity of the flows involved and the need to test at adequate Reynolds numbers and at the correct Mach number. An example of the spanwise optimisation of a leading device is given and some results showing the variation of $C_{L_{max}}$ on a finite high lift wing when Reynolds number and Mach number were varied independently, are commented upon.

Finally a technique for developing practical slat and flap track support systems using a large swept end-plate model is described and some results given showing the improvements made to a particular flap track system.

2. THEORETICAL PROCEDURES

2.1 Two-dimensional Theory

The starting point of research and development of new high lift devices usually takes the form of a theoretical appraisal, mainly two-dimensional, using initially the simpler inviscid surface singularity techniques. This is followed by refinement using viscous theory either to provide a simple displacement surface correction or to obtain a fully iterative viscous solution as in the R.A.E. method M.A.V.I.S.[1] (Multiple Aerofoil Viscous Iterative Solution).

The inviscid surface singularity method originally due to Hess and Smith[2] still provides a surprisingly good initial design. Figure 1 shows a slat and single slotted flap designed using this method, and the agreement with experiment is quite good. Improved versions of the basic method are now available[3].

An example of the use of this method, including some viscous calculations to design a particular form of Kruger slat can be given. This slat, called a rigid camber Kruger, was devised by B.Ae., Weybridge to avoid the complexity and weight of the Boeing variable camber Kruger and is shown in Figure 2. The first geometry, (K13) was designed using the inviscid theory while the second (L9) was developed using viscous theory, non-iteratively (see figure 3). Figure 4 shows how the pressure distribution of L9 was changed from that of a more conventional distribution to give a Stratford type of gradient, with separation values of $\bar{H}$ being delayed until near the trailing edge of the slat.

2.2 Viscous Iterative Theory

The prediction of $C_{L_{max}}$ and drag is impossible without a fully iterative viscous interaction theory and in the U.K. the R.A.E. have developed such a theory in two dimensions with M.A.V.I.S.,[1] based on Irwin's[4] wake model. Figure 5 shows the basic physical model, with boundary layers and wakes interacting. B.Ae. Woodford Division, are developing an improved version where the boundary layers are represented by transpiration. An example of the use of the method is shown in figure 6 where the calculated pressures on an aerofoil with slat and single slotted flap are in good agreement with experiment. B.Ae. are making increasing use of the method to design new high lift devices.

2.3 Three-dimensional Theory

To design high lift devices for finite wings a three-dimensional theory is necessary. Woodward[5] has shown that for a trapezoidal wing, the pressure distribution at mid span is equivalent to that of the corresponding two-dimensional section using a simple normalisation process.

If the geometrical correspondence of the high lift sections is such that, for $(x/c)_{swept} = (x/c)_{2D}$

$$(Z/c)_{swept} = (Z/c)_{2D} \cos\phi_1 \qquad (1)$$

then

$$Cp_{swept} = Cp_{2D} \cos^2\phi_1 \qquad (2)$$

where ϕ_1 is the local sweep angle, and 2D refers to two-dimensional conditions.

The success of the theory is demonstrated experimentally in figure 7 using results from the U.K. National High Lift Programme

The normalisation theory leads to the idea that the pressure on a more general three dimensional wing can be predicted by a quasi two-dimensional approach in which the three-dimensional effects are included as an onset flow. This onset flow can be split into two components, a uniform distribution across the chord which can be obtained by normalising the pressure distributions and geometry as described above, and a non-uniform distribution which can be calculated using panel methods such as the B.Ae. Hunt-Semple method[6].

Figure 8 shows the procedure schematically, where the slat and flap slots are faired in to simplify the panel method calculations. The procedure has the great advantage that all the advances made in two-dimensional theory such as M.A.V.I.S. can be utilised, avoiding the severe complexities of a fully three-dimensional approach. Calculations of this type already done by Hardy at R.A.E. suggest that for a moderate aspect ratio wing of constant section and thickness the non-uniform onset flow is relatively small over most of the span.

3. EXPERIMENTAL TECHNIQUE-TWO DIMENSIONS.

Although theoretical methods are playing an increasing part in high lift design, wind tunnel experiments still play an essential role. The final choice of high lift devices and their grading across the span requires sectional testing at high Reynolds numbers. Part of the U.K. National High Lift Programme involved the design and testing by the B.Ae. Weybridge Division of a wide variety of conventional and advanced high lift devices in a consistent environment. This was done by developing a two-dimensional model and a related quasi two dimensional End-Plate model, and testing at a fixed Reynolds number of about 4.5×10^6 and a constant Mach number of 0.18.

3.1 Two-dimensional Model

A photograph of the two-dimensional model in the Weybridge 4.0m x 2.8m low speed tunnel is shown in figure 9. To remove the substantial wall boundary layer, wall suction was employed as shown in figure 10. Chordwise pressure measurements at the tunnel centre-line and roof proved that the flow was substantially two-dimensional (see figure 11). The aerofoil section was of 'Airbus' type and four main configurations tested as shown in figure 12; an overwing slat with single double and triple-slotted flaps and a Kruger slat with the triple-slotted flap.

Variations of slat and flap lap and gap geometry were tested on most of the configurations, lift being measured by pressure integration and drag by wake traverse measurements downstream of the model. As an example, the effect on C_{Lmax} and drag of changing slat gap is given in figure 13, the best C_{Lmax} position not quite coinciding with the lowest profile drag position. In a number of cases total head measurements were made in the viscous layers, a typical result being shown in figure 14. This data has been invaluable in developing two-dimensional theoretical methods.

3.2 Quasi Two-dimensional Model

To reduce the cost and time of testing, a quasi two-dimensional model was obtained by reducing the span of the two-dimensional model from 2.8m to 2.3m and fitting large end-plates. A photograph of this model is given in figure 15, and its planform geometry can be seen in figure 16. There are pressure plotting stations at the centre-line and near one end-plate and figure 17 shows that the pressure distributions measured at these two stations are in close agreement, confirming that the flow over the end-plate model is essentially two-dimensional in character.

When centre-line pressure distributions on the two models are compared (figure 18) at the same value of C_N, that is at similar values of effective incidence, the pressure distributions are very nearly the same. The downwash induced by the end-plates causes a slight increase in slat suction, with pressures on the wing and flap scarcely affected. Viscous shear layer measurements on both types of model also showed very good agreement when compared at the same effective incidence.

3.2 Correction of End-plate Results

The fact that the pressure distributions agreed so well at the same C_N suggested that a simple mean induced incidence correction might convert the end-plate results to essentially two-dimensional conditions

$$\text{Assume } \bar{\alpha}_i = \tan^{-1} KC_L \quad (3)$$

$$\text{then } C_{L_2} = C_L(EP)\cos\bar{\alpha}_i + C_D(EP)\sin\bar{\alpha}_i \quad (4)$$

$$C_{D_2} = C_D(EP)\cos\bar{\alpha}_i - C_L(EP)\sin\bar{\alpha}_i \quad (5)$$

where (EP) refers to balance forces measured on the end-plate model and suffix 2 refers to two-dimensional conditions (see figure 19). If the value of K in equation 3 remains constant for a number of widely different high lift configurations then the simple correction method will work. That this is so is shown in figures 19 and 20. Four widely differing high lift configurations had been tested on both two-dimensional and end-plate models, including single, double and triple slotted flaps with slats and Krugers, and a single value of K was found which gave a very good collapse of the lift curves as will be seen in figure 19. When allowance is made for the end-plate rig drag the drag curves are also seen to agree (figure 20). A fuller discussion of the theory is given in a B.Ae. report.(7).

3.4 U.K. Two-dimensional Research

As part of the U.K. National High Lift Programme (N.H.L.P.) which started in 1970, B.Ae., Weybridge carried out tests, using both types of model on a wide variety of conventional and advanced high lift devices, and new devices are currently being developed. A large body of data has been amassed, all tested under identical conditions. Reynolds number was held constant at $R_e = 4.5 \times 10^6$ and Mach number at $M = 0.18$, and the importance of this will be referred to later. Figures 21 and 22 give an indication of the range of leading and trailing edge devices tested. Besides testing a number of deflection angles, the lap and gap geometry of most devices has also been varied to establish optimum configurations. The list includes single and double slotted flaps with different chord and shroud lengths, triple slotted flaps and conventional and Kruger slats. The most complete current index of tests is given in a B.Ae. report.(8).

3.5 Some Comparisons of High Lift Devices

From the data obtained in the N.H.L.P accurate comparisons of different high lift devices can be made and a few examples are given here. Conventional over-wing slats and Kruger slats are compared, an externally hinged flap is compared with a tracked flap system and the effect of supercritical aerofoil profile features is shown.

The results of comparing over-wing slats and variable camber Kruger slats which retract into the aerofoil lower surface are shown in figure 23. Due partly to its greater extended chord and better leading edge shape the Kruger has a greater maximum lift and its profile drag for a given maximum lift is less.

The geometry of an externally hinged flap system is compared, (figure 24), with that of a similar tracked flap system which allows more rearward extension. The results of the comparison of C_{Lmax} is given in figure 25. When compared on datum reference chord, the hinged flap (T10) C_{Lmax} is lower due to its lack of extension, but when compared on the truer aerodynamic basis of extended

chord T10 is just as efficient as the tracked system at its design angles of 20^{o} and 45^{o}. At all other intermediate angles however, T10 is much less efficient. This trend can also be observed in the lift-drag performance comparison of figure 26.

The datum aerofoil was modified as shown in figure 27 to incorporate the main geometrical features of a more advanced supercritical section. The comparison was made in two stages, (figure 28). The first, involving only the modification moving the position of minimum upper surface curvature back, showed a small loss (1%) in C_{Lmax}. The second stage, this time in the presence of a variable camber Kruger slat appears to suggest that the full supercritical profile with its larger leading edge radius, has offset even this small loss, to give no loss of C_{Lmax}. It should be noted however that the datum flap T2 has been used through-out this comparison.

These examples show how B.Ae. is able to use the two-dimensional technique to select the appropriate devices for a particular project.

4. THREE DIMENSIONAL EXPERIMENT

Although the initial selection of high lift devices can be made from two-dimensional theory and test, the final optimisation spanwise can only be done at present by three-dimensional testing on the actual aircraft geometry. In spite of the promising developments in quasi three-dimensional theory referred to earlier, the task of predicting C_{Lmax} and drag theoretically on finite high lift wings is a formidable one. The immense complexity of the flow at the stall is illustrated in figures 29 and 30 where a relatively small change in spanwise extent of the slat at the wing root has caused a completely different pattern of flow breakdown, and a big gain in C_{Lmax}.

4.1 Spanwise Optimisation

An example of optimisation in three-dimensions is given in figures 31 and 32 illustrating the need to compromise between aerodynamic efficiency and stall control. A B.A.C. 1-11 wing was tested initially with a full span sealed Kruger in the B.Ae. Weybridge 4.0m x 2.8m tunnel. Because of unacceptable wing-dropping characteristics at the stall, the outer slat segment was vented to delay the outer wing stall. (See figure 31). However, figure 32 shows that there was a drag penalty to be paid in achieving the better stall control.

4.2 High Reynolds Number Testing

These final three-dimensional optimisations should of course be done at adequate Reynolds numbers and the correct Mach number. In the U.K., industry is making increasing use of the new R.A.E. 5m low speed tunnel which can be pressurised up to 3 bars. Figure 33 shows a model of the A300 in this tunnel, which achieves a Reynold number of 6×10^{6} at $M = 0.18$.

Basic high lift research in the 5m tunnel is also being carried out on such models as R.A.E. Model 477, (figure 34) which has the same section and devices as the B.Ae. Weybridge two-dimensional models, as well as having variable sweep-back. Significant Reynolds number and Mach number effects on C_{Lmax} have been demonstrated (figure 35) on this model. These results suggest that since the stall occurs on the outer wing, the Reynolds number effects on C_{Lmax} are substantially over when the tip Reynolds number exceeds a value of between 3 and 4×10^{6}. This implies that there is likely to be little further Reynolds number effect on the C_{Lmax} of the bank of two-dimensional data referred to in earlier sections of the paper, thus increasing the confidence in the use of this data as representing near full scale C_{Lmax} conditions. Drag of course will continue to vary up to the actual full scale Reynolds number.

To exploit further, the advantages of the R.A.E. 5m Wind tunnel, B.Ae. is designing and manufacturing a large scale half-model representative of projected advanced technology civil transports for test in 1981/2.

5. SLAT AND FLAP TRACK DEVELOPMENTS

The final element in the B.Ae. Weybridge design procedure is the detailed development of practical flap and slat support system. Theory is of little use here and a large scale rig is necessary to obtain high Reynolds numbers and to achieve the physical scale necessary to represent all the details of what are necessarily complex mechanical systems. A large scale swept end-plate model (figure 36) has been developed at Weybridge for studying the detailed aerodynamic effects of flap tracks, flap track fairings and slat rails. A photograph of a typical flap track development test geometry is shown in figure 37.

An example of the use of this technique can be quoted in the development of improved flap track fairings for the B.A.C. 1-11. Figure 38(a), shows the original flap track fairings, while figure 38(b) shows the revised flap

track fairing after development on the swept end-plate model. The model tests showed a significant reduction in flap drag and this was confirmed in the subsequent flight test checks, as shown in figure 39. This technique will continue in use, since the scale of models designed for pressurised high Reynolds number wind tunnels will generally be too small for adequate representation of mechanical detail.

6. CONCLUSIONS

This paper has attempted to summarise the procedures used by the Weybridge-Bristol Division of British Aerospace to design high lift devices for civil transport aircraft.

The theoretical methods, both two- and three-dimensional are discussed and the importance of using a fully interactive viscous solution is stressed. An example of the design process is given, the design being that of a rigid camber Kruger slat.

The experimental techniqus are next discussed, showing the value of systematic testing, at adequate Reynolds number, on large two-dimensional models. This technique, which was used in part of the U.K. National High Lift Programme, has led to the acquistion of a large body of consistent data for a wide variety of conventional and advanced high lift devices. It enables the appropriate high lift system to be chosen (or a new one to be developed) for a particular project, and examples of comparisons of different devices are given. These include comparisons between an over-wing and a Kruger slat, and between an externally hinged and a tracked flap system; the effect of supercritical aerofoil profiles on high lift performance is also shown.

The three-dimensional experimental techniques used are next reviewed, an example of spanwise Kruger slat optimisation being shown. The need to test at adequate Reynolds numbers is stressed, and it is suggested that large pressurised high Reynolds number tunnels such as the R.A.E. 5m low speed tunnel will increasingly be used in the high lift design process.

REFERENCES

1. B.R. Williams, D.S. Woodward: Multiple-Aerofoil Viscous Iterative System (M.A.V.I.S.). - The initial structure and possible extensions. Unpublished M.o.D. Report, 1975

2. J.L. Hess, A.M.O. Smith: Calculation of Potential Flow about Arbitrary Bodies. - Progress in Aeronautical Science, Vol. 8. Pergamon Press, 1966.

3. J.C. Newling: An improved two-dimensional multi-aerofoil program. Unpublished B.Ae. Report, 1977.

4. H.P.A.H. Irwin: A calculation method for the two-dimensional flow over a slotted flap. R.A.E. TR 72124, 1972.

5. D.S. Woodward: National High Lift Programme - an interim report and view of the future. Unpublished M.o.D. Report, 1975.

6. B. Hunt, W.G. Semple: The panel method for subsonic aerodynamic flows - a survey of mathematical formulation and numerical models and an outline of the new British Aerospace scheme. V.K.I. Lecture Series, 1978.

7. J.R. Wedderspoon: Prediction of two-dimensional lift and drag data from end-plate model tests. Unpublished B.Ae. Report, 1977.

8. B.S.P. Finch: A review of N.H.L.P. quasi two-dimensional end-plate testing at B.Ae. Weybridge, over the period 1969 to 1979. Unpublished B.Ae. Report, 1980.

Note: Reports quoted as references are not necessarily available to members of the public or to commercial organisations.

ACKNOWLEDGMENT

The author wishes to thank British Aerospace, the Ministry of Defence (P.E.) and R.A.E. for permission to use some of the material contained in this paper.

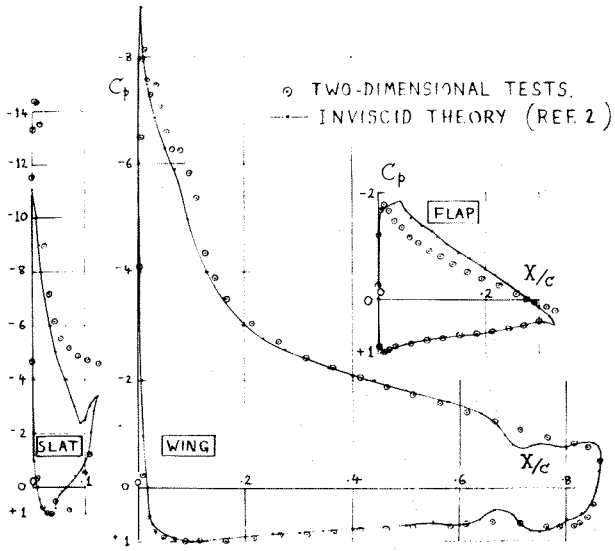

FIG. 1 INVISCID THEORY AND EXPERIMENT FOR AN AEROFOIL WITH SLAT AND FLAP.

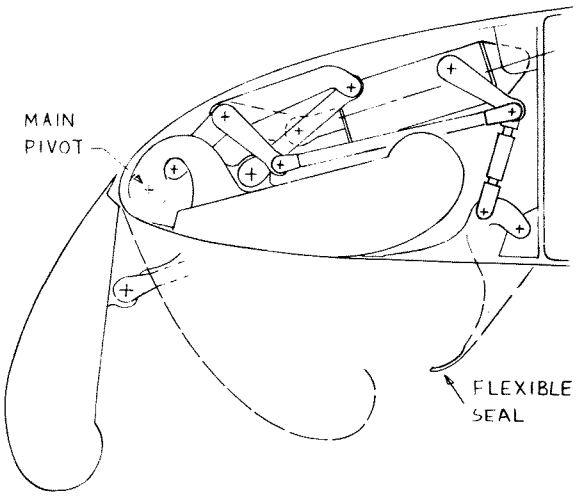

FIG. 2 RIGID CAMBER KRUGER SLAT

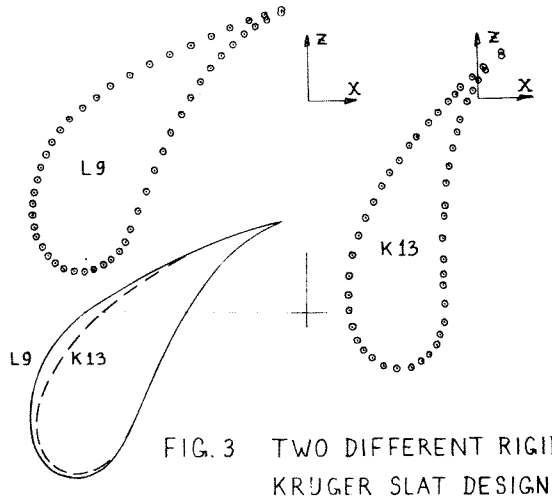

FIG. 3 TWO DIFFERENT RIGID KRUGER SLAT DESIGNS.

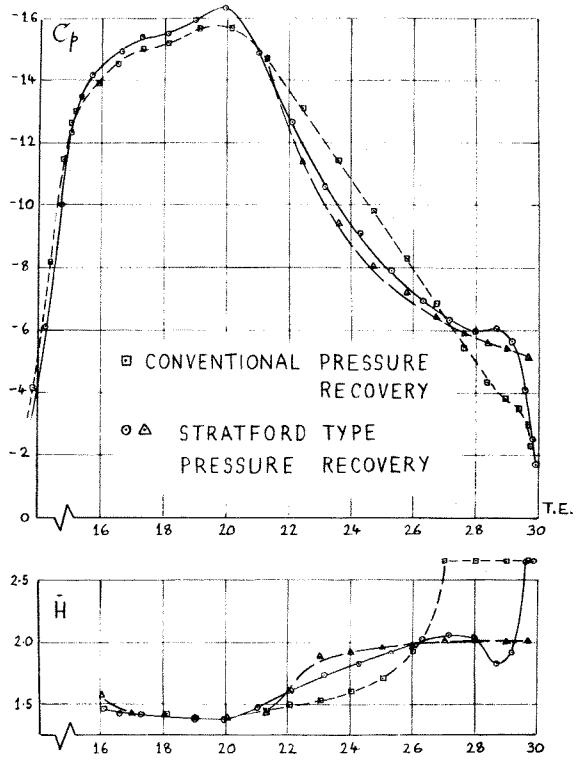

FIG. 4 THEORETICAL PRESSURE AND $\bar{H}$ DISTRIBUTIONS FOR THE KRUGER SLAT L9.

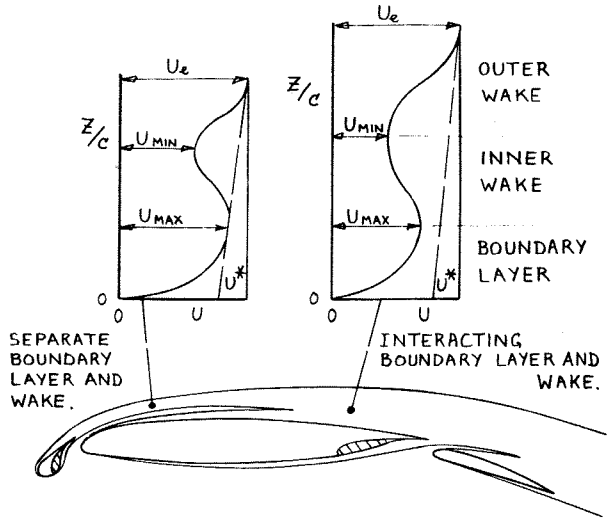

FIG. 5 VISCOUS THEORETICAL MODEL USED IN M.A.V.I.S. THEORY

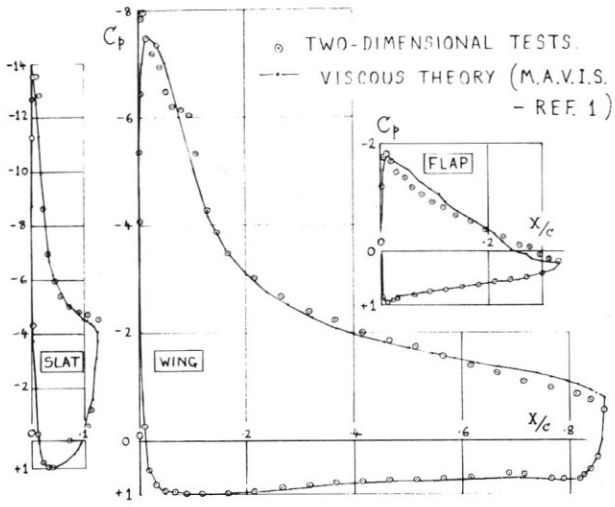

FIG. 6 VISCOUS THEORY AND EXPERIMENT FOR AN AEROFOIL WITH SLAT AND FLAP.

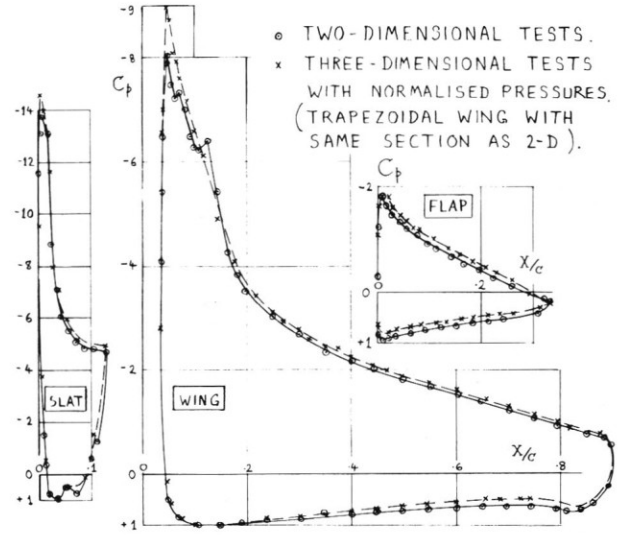

FIG. 7 COMPARISON OF TWO DIMENSIONAL AND NORMALISED THREE DIMENSIONAL PRESSURES.

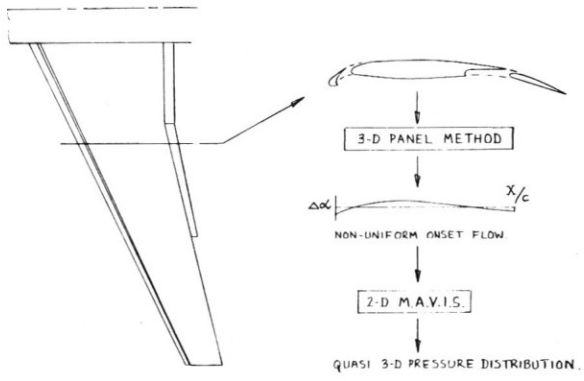

FIG. 8 QUASI THREE-DIMENSIONAL THEORETICAL METHOD.

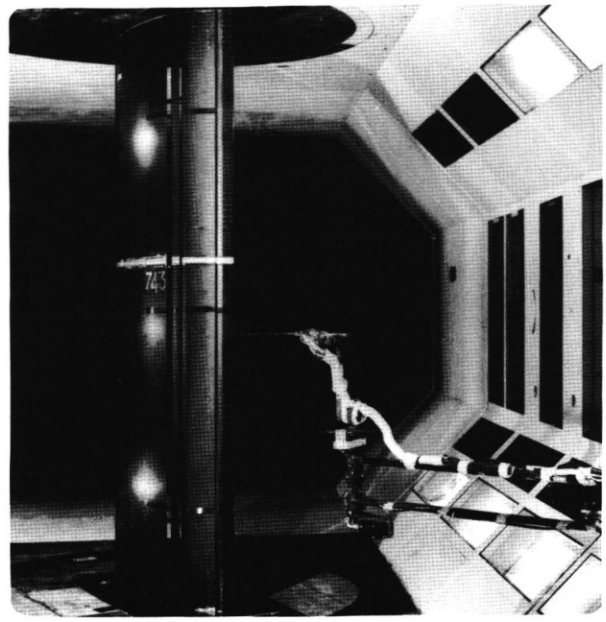

FIG. 9 B.Ae. WEYBRIDGE TWO-DIMENSIONAL MODEL.

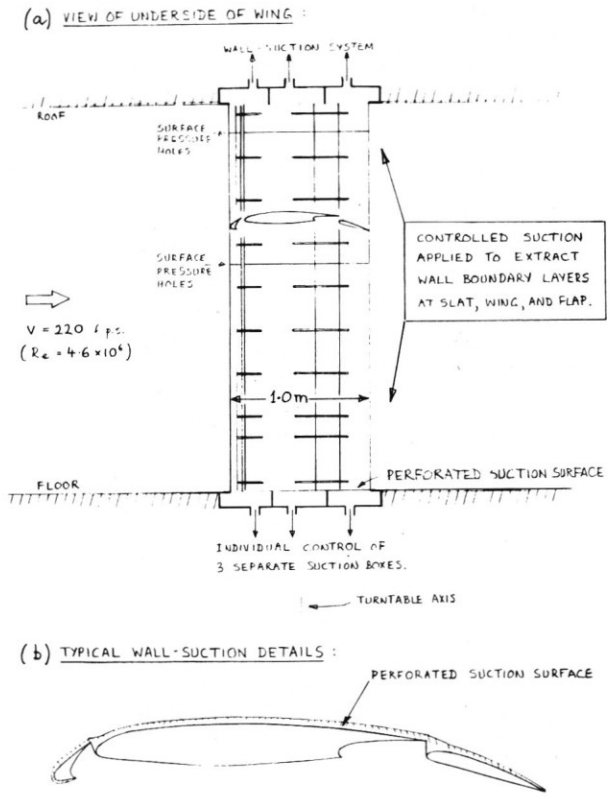

FIGURE 10 : 2-D MODEL WITH WALL SUCTION

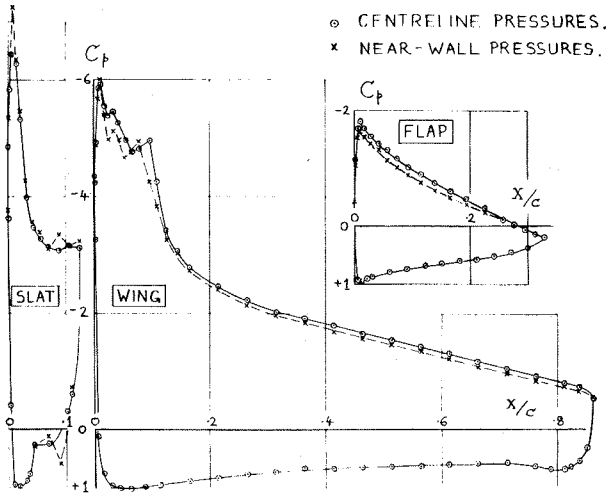

FIG. 11 PRESSURES AT CENTRELINE AND NEAR WALL OF TWO-DIMENSIONAL MODEL.

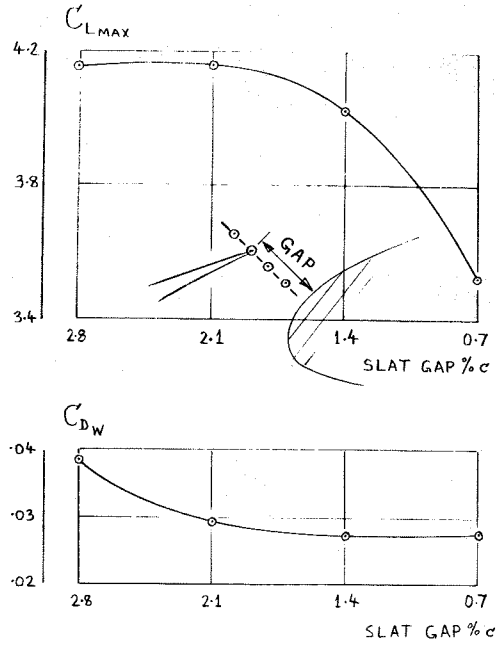

FIG. 13 EFFECT OF GAP VARIATION ON TWO-DIMENSIONAL MODEL.

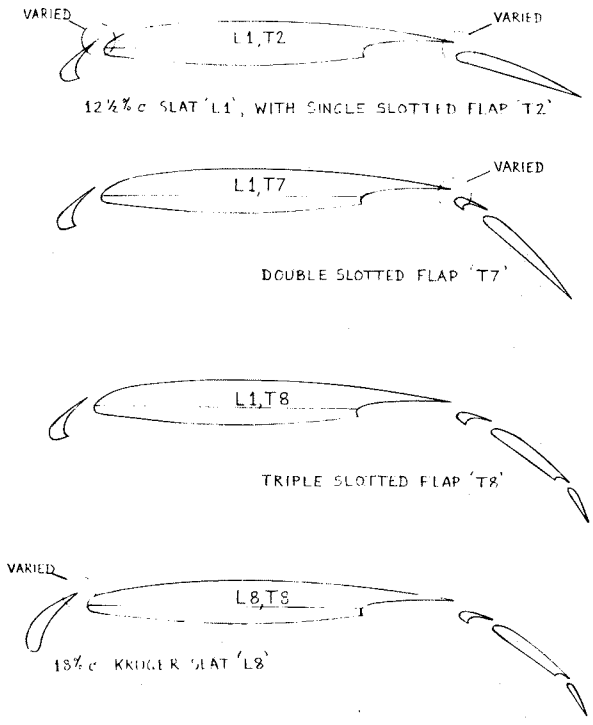

FIGURE 12: 2-D MODEL WITH WALL SUCTION FOUR MAIN HIGH LIFT TEST CONFIGURATIONS.

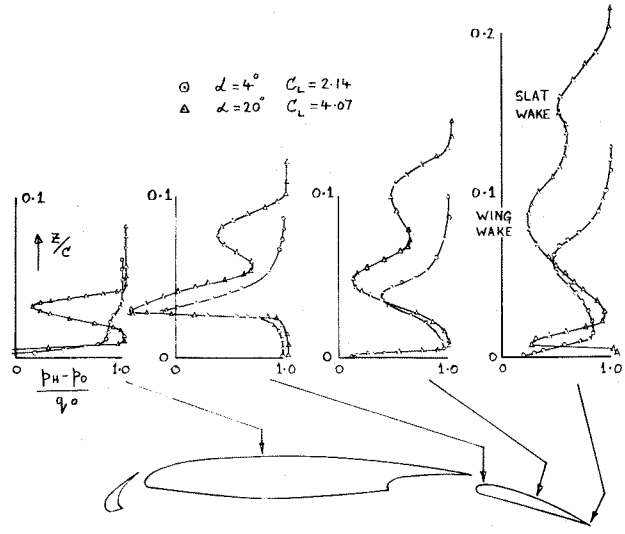

FIG. 14 VISCOUS LAYER PROFILES ON TWO-DIMENSIONAL MODEL.

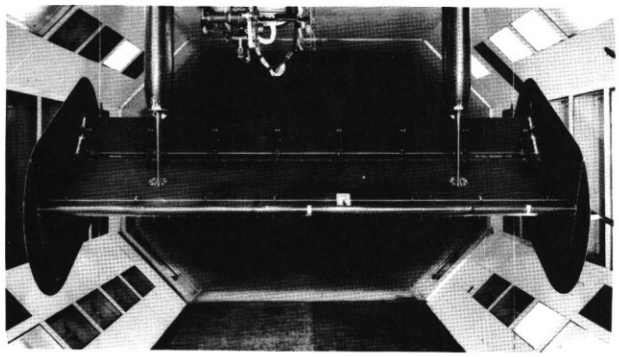

FIG. 15 B.Ae. WEYBRIDGE END-PLATE MODEL.

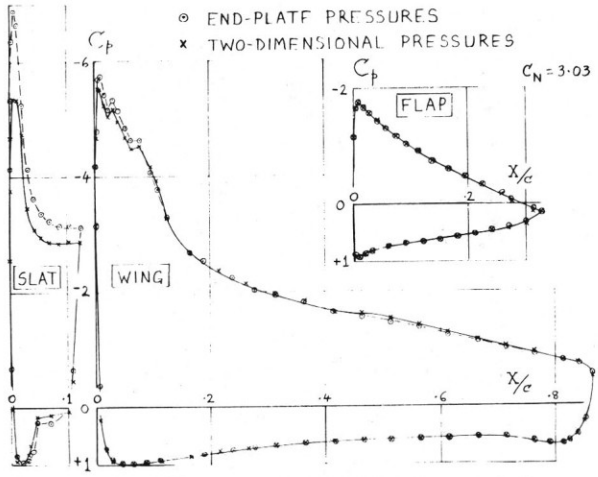

FIG. 18 CENTRELINE PRESSURES ON 2-D AND END-PLATE MODELS.

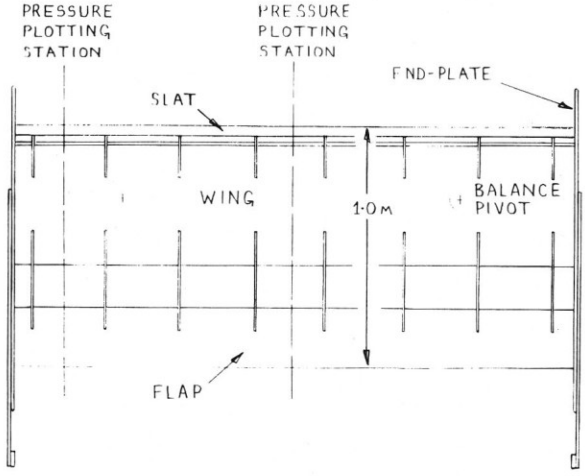

FIG. 16 QUASI TWO-DIMENSIONAL END-PLATE MODEL.

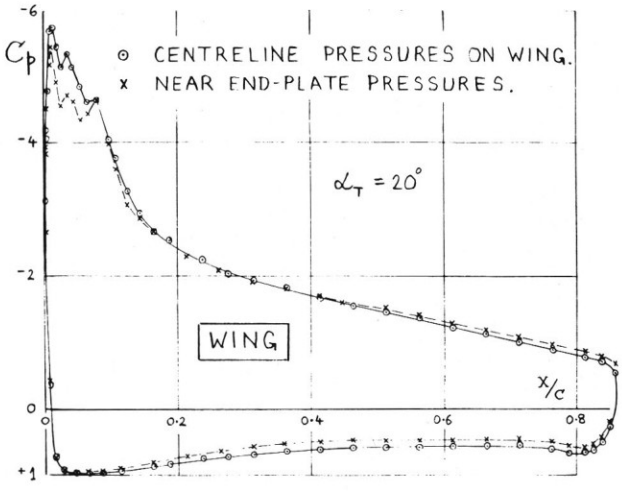

FIG. 17 PRESSURES AT CENTRELINE AND NEAR END-PLATE — MODEL WITH SLAT AND FLAP

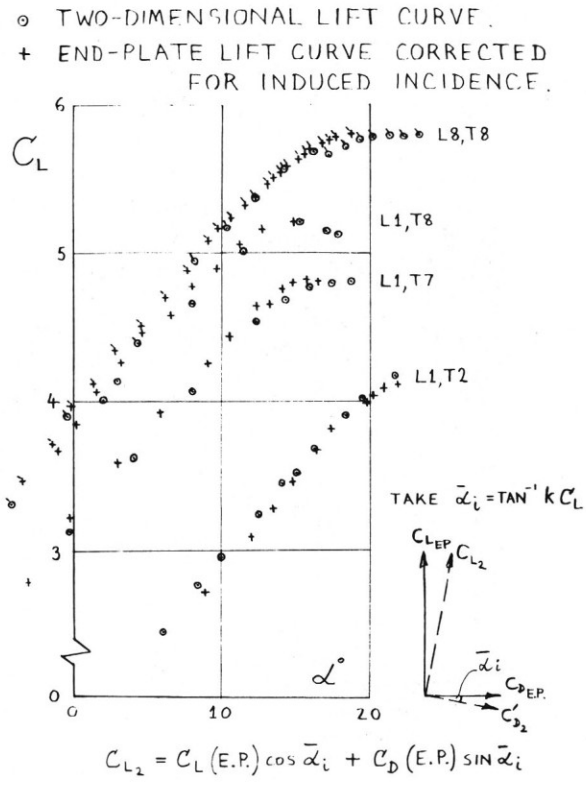

FIG. 19 COMPARISON OF 2-D AND CORRECTED END-PLATE LIFT CURVES.

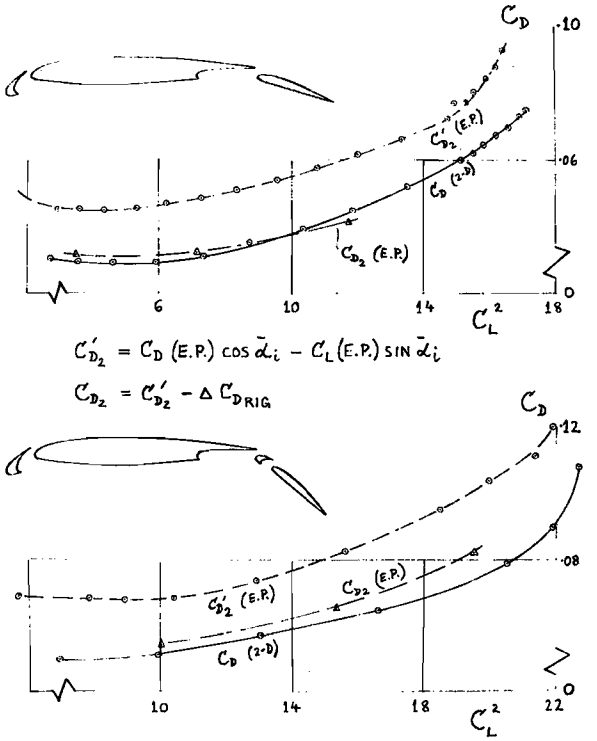

FIG. 20 COMPARISON OF 2-D AND CORRECTED END-PLATE DRAG.

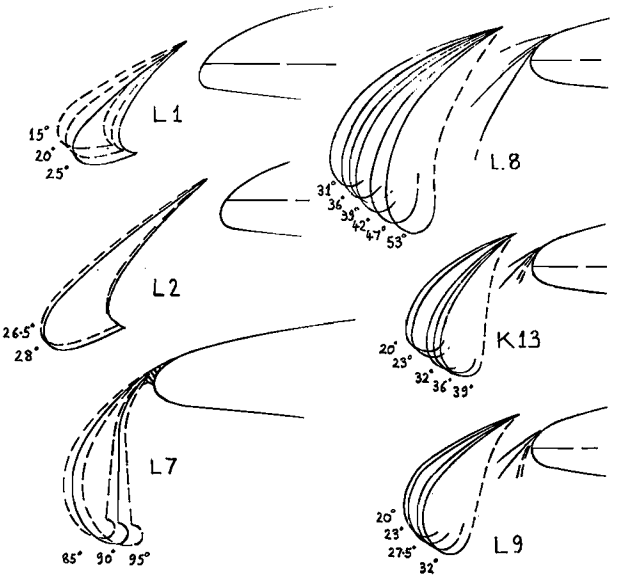

FIG. 22 LEADING EDGE DEVICES TESTED IN U.K. NATIONAL HIGH LIFT PROGRAMME.

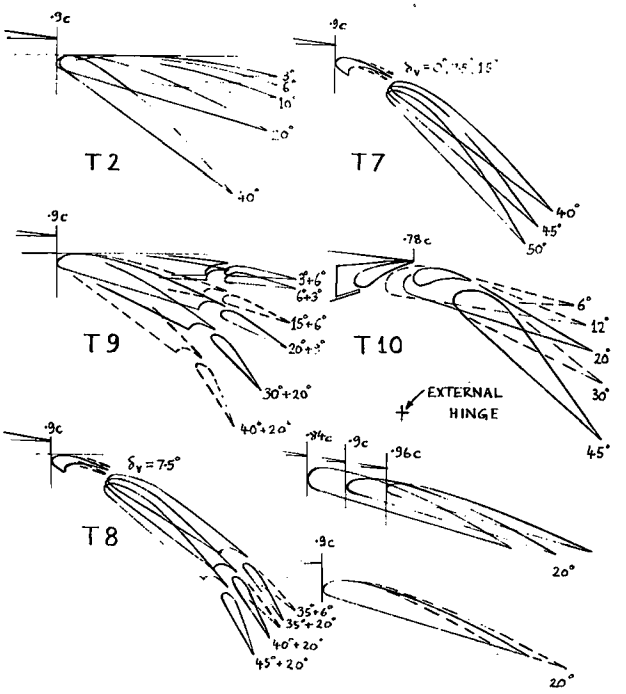

FIG. 21 TRAILING EDGE DEVICES TESTED IN U.K. NATIONAL HIGH LIFT PROGRAMME.

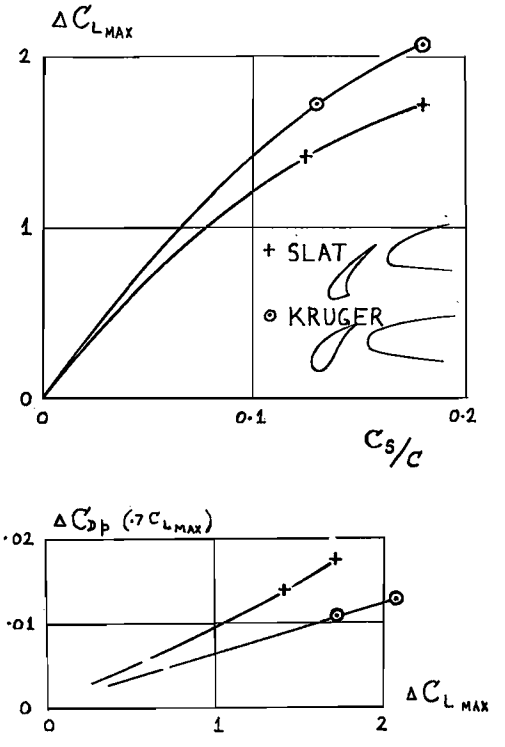

FIG. 23 COMPARISON OF OVER-WING SLAT AND KRUGER SLAT.

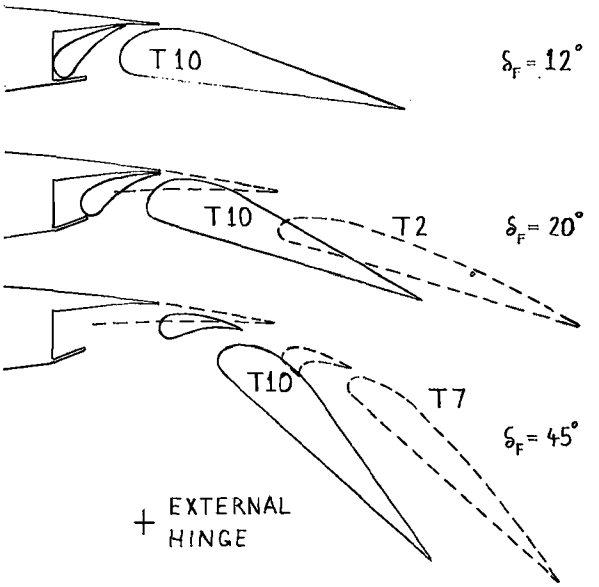

FIG. 24 COMPARISON OF EXTERNALLY HINGED FLAP AND TRACKED FLAP GEOMETRY.

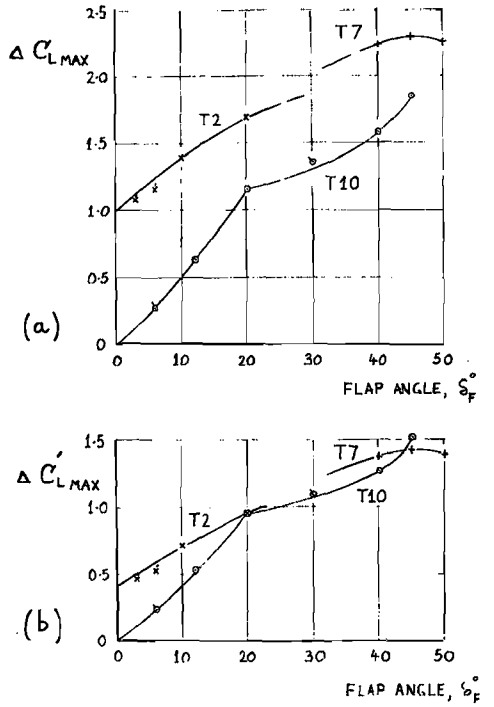

FIG. 25 COMPARISON OF EXTERNALLY HINGED FLAP AND TRACKED FLAP SYSTEM
(a) BASED ON DATUM REFERENCE CHORD
(b) BASED ON EXTENDED CHORD.

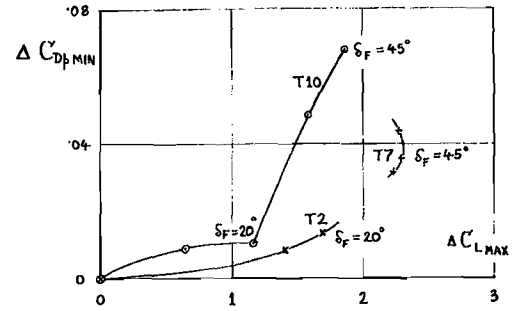

FIG. 26 LIFT-DRAG PERFORMANCE COMPARISON OF EXTERNALLY HINGED FLAP AND TRACKED FLAP SYSTEM.

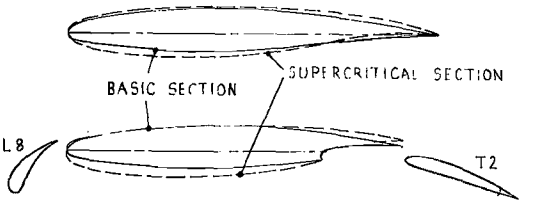

FIG. 27 GEOMETRY OF BASIC SECTION WITH SUPERCRITICAL PROFILE MODIFICATIONS.

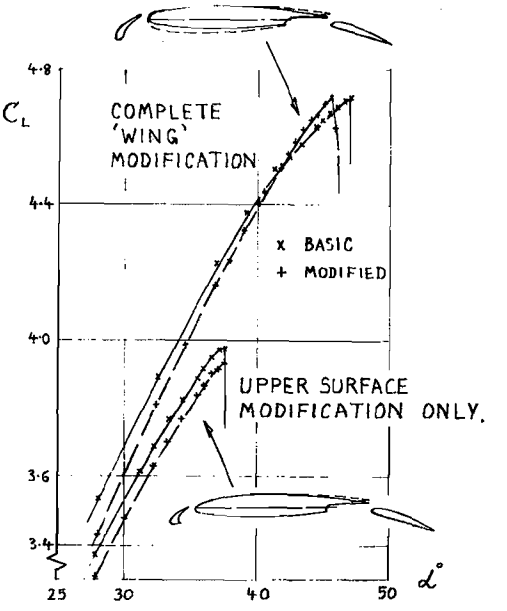

FIG. 28 COMPARISON OF THE EFFECTS OF MODIFYING DATUM SECTION TO 'SUPERCRITICAL' PROFILE.

FIG. 29 WING ROOT FLOW AT STALL— 90% SPAN SLAT.

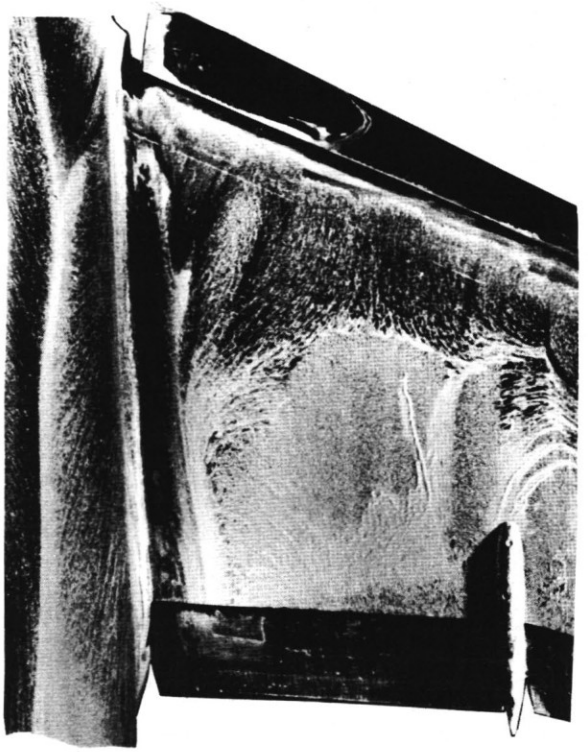

FIG. 30 WING ROOT FLOW AT STALL— 100% SPAN SLAT.

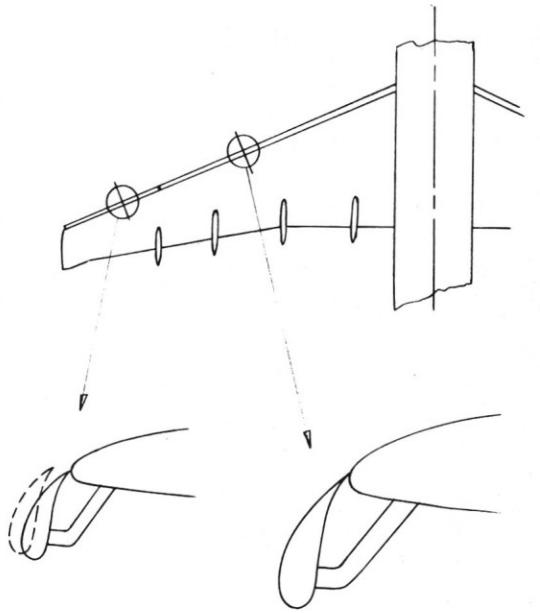

FIG. 31 THREE DIMENSIONAL SLAT VARIATION — GEOMETRY.

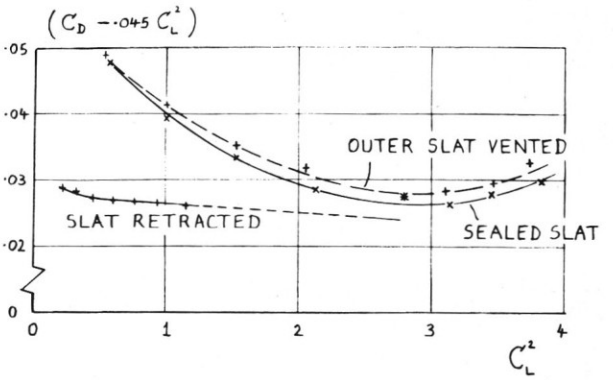

FIG. 32 EFFECT OF SLAT GEOMETRY VARIATIONS ON PROFILE DRAG.

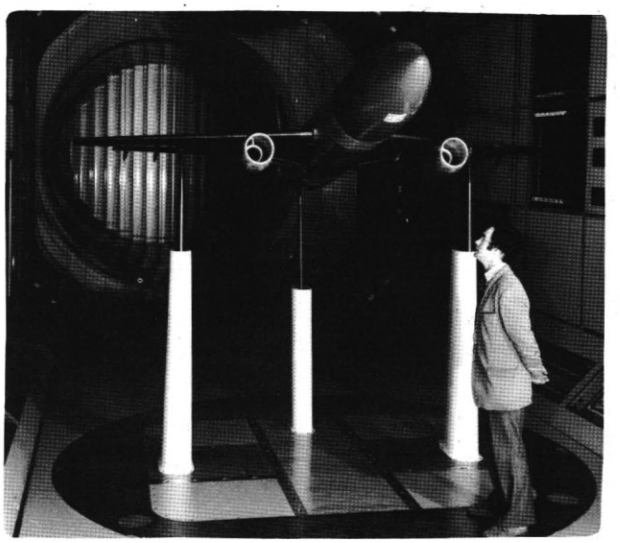

FIG. 33 A300 MODEL IN R.A.E. 5m. LOW SPEED WIND TUNNEL.

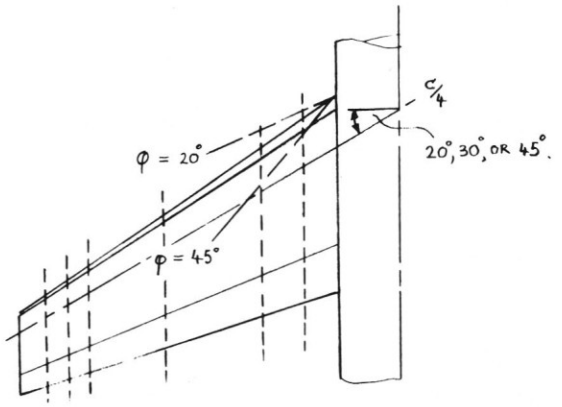

FIG. 34 R.A.E. MODEL 477 GEOMETRY.

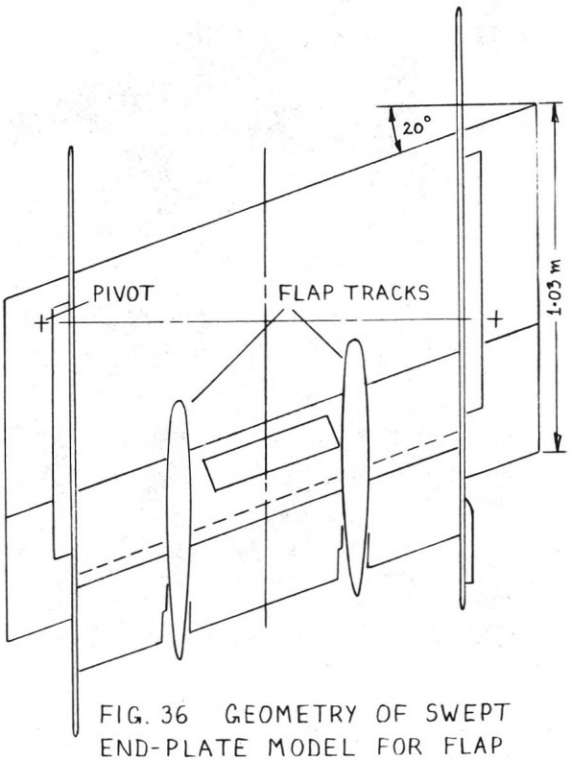

FIG. 36 GEOMETRY OF SWEPT END-PLATE MODEL FOR FLAP TRACK SYSTEM DEVELOPMENT.

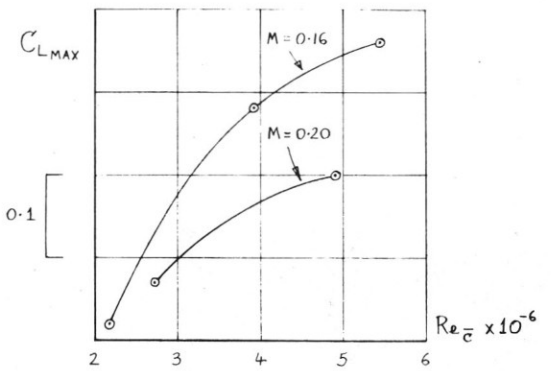

FIG. 35 EFFECT OF Re No. AT CONSTANT MACH No. ON MODEL 477.

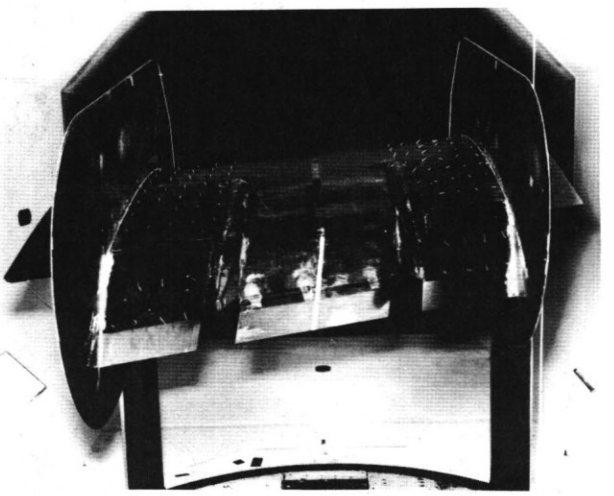

FIG. 37 TYPICAL FLAP TRACK DEVELOPMENT TEST.

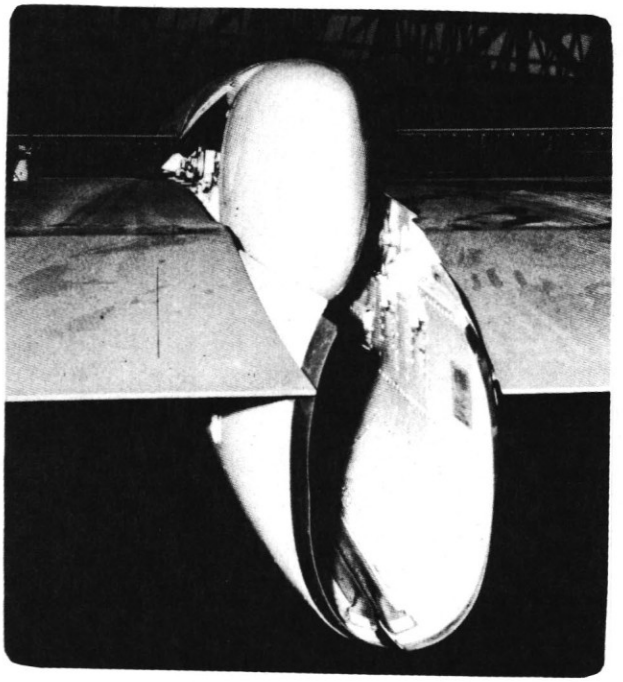

FIG. 38 (a) ORIGINAL FLAP TRACK FAIRING.

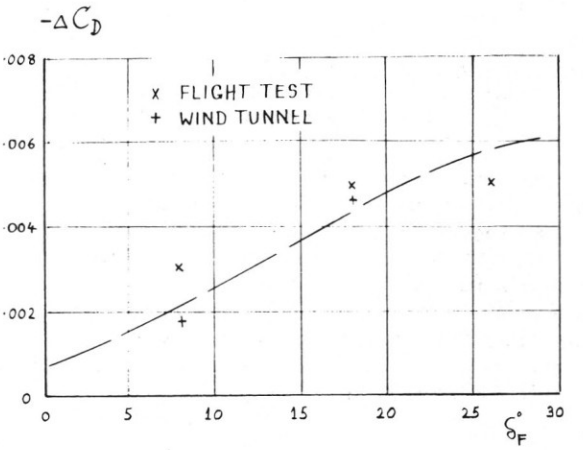

FIG. 39 DRAG REDUCTION DUE TO IMPROVED FLAP TRACK SYSTEM ON B.A.C. 1-11 .

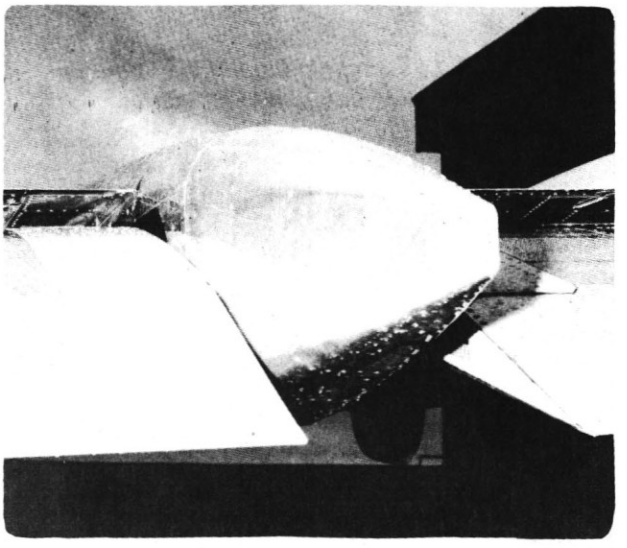

FIG. 38 (b) MODIFIED FLAP TRACK FAIRING.